THE ASTROPHYSICAL JOURNAL, 475:429–444, 1997 February 1

21 CENTIMETER TOMOGRAPHY OF THE INTERGALACTIC MEDIUM AT HIGH REDSHIFT

PIERO MADAU
Space Telescope Science Institute, 3700 San Martin Drive, Baltimore, MD 21218; madau@stsci.edu
AVERY MEIKSIN[1]
Department of Astronomy and Astrophysics, University of Chicago, 5640 South Ellis Avenue, Chicago, IL 60637; meiksin@oddjob.uchicago.edu
AND
MARTIN J. REES
Institute of Astronomy, Madingley Road, Cambridge CB3 0HA, UK
Received 1996 February 9; accepted 1996 August 26

ABSTRACT

We investigate the 21 cm signature that may arise from the intergalactic medium (IGM) prior to the epoch of full reionization ($z > 5$). In scenarios in which the IGM is reionized by discrete sources of photoionizing radiation, the neutral gas that has not yet been engulfed by an H II region may easily be preheated to temperatures well above that of the cosmic background radiation (CBR), rendering the IGM invisible in absorption against the CBR. We identify three possible preheating mechanisms: (1) photoelectric heating by soft X-rays from QSOs, (2) photoelectric heating by soft X-rays from early galactic halos, and (3) resonant scattering of the continuum UV radiation from an early generation of stars. We find that bright quasars with only a small fraction of the observed comoving density at $z \sim 4$ will suffice to preheat the entire universe at $z \gtrsim 6$. We also show that, in a cold dark matter dominated cosmology, the thermal bremsstrahlung radiation associated with collapsing galactic mass halos (10^{10}–$10^{11}\ M_{\odot}$) may warm the IGM to $\sim$100 K by $z \sim 7$. Alternatively, the equivalent of $\sim$10% of the star formation rate density in the local universe, whether in isolated pregalactic stars, dwarf, or normal galaxies, would be capable of heating the entire IGM to a temperature above that of the CBR by Lyα scattering in a small fraction of the Hubble time at $z \sim 6$.

In the presence of a sufficiently strong ambient flux of Lyα photons, the hyperfine transition in the warmed H I will be excited. A beam differencing experiment would detect a patchwork of *emission*, both in frequency and in angle across the sky. This patchwork could serve as a valuable tool for understanding the epoch, nature, and sources of the reionization of the universe, and their implications for cosmology. We demonstrate that isolated QSOs will produce detectable signals at meter wavelengths within their "spheres of influence" over which they warm the IGM. As a result of the redshifted 21 cm radiation emitted by warm H I bubbles, the spectrum of the radio extragalactic background will display frequency structure with velocity widths up to 10,000 km s^{-1}. Broad beam observations would reveal corresponding angular fluctuations in the sky intensity with $\delta T/T \lesssim 10^{-3}$ on scales $\theta \sim 1°$. This scale is set either by the "thermalization distance" from a QSO within which Lyα pumping determines the spin temperature of the IGM or by the quasar lifetime.

Radio measurements near 235 and 150 MHz, as will be possible in the near future using the Giant Metrewave Radio Telescope, may provide the first detection of a neutral IGM at $5 \lesssim z \lesssim 10$. A next generation facility like the Square Kilometer Array Interferometer could effectively open much of the universe to a direct study of the reheating epoch and possibly probe the transition from a neutral universe to one that is fully ionized.

Subject headings: cosmology: theory — diffuse radiation — intergalactic medium — quasars: general — radio lines: general

1. INTRODUCTION

At epochs corresponding to $z \sim 1000$, the intergalactic medium (IGM) is expected to recombine and remain neutral until sources of radiation develop that are capable of reionizing it. The application of the Gunn-Peterson (1965) constraint on the amount of cosmologically distributed neutral hydrogen to QSO absorption spectra requires the universe to have been highly ionized by $z \sim 5$ (Schneider, Schmidt, & Gunn 1991). It thus appears that substantial sources of ionization were present at these or earlier epochs, perhaps QSOs and young galaxies, or some as yet undiscovered class of objects such as Population III stars or decaying particles. Establishing the epoch of reionization is crucial for determining the impact of reionization on several key cosmological issues, from the role reionization plays in allowing collapsed objects to cool and make stars, to determining the small-scale structure in the temperature fluctuations of the cosmic background radiation (CBR) (e.g., Sugiyama, Silk, & Vittorio 1993; Hu & White 1996). Conversely, probing the epoch of reionization may provide a means of detecting the onset of the first generation of stars.

Very little is known about the nature of the first bound objects and of the thermal state of the universe at early epochs. In particular, the history of the transition from a

[1] Edwin Hubble Research Scientist.

neutral IGM to an almost fully ionized one can reveal the character of the ionizing sources. If these are uniformly distributed, like an abundant population of pregalactic stars or decaying dark matter, the ionization and thermal state of the IGM will be the same everywhere at any given epoch, with the neutral fraction decreasing gradually with cosmic time. In a cold dark matter (CDM) dominated cosmology, this may be the case since bound objects sufficiently massive ($\sim 10^6\ M_\odot$) to make stars form at high redshift. If a sufficient fraction of their ionizing photons are able to escape, the stars in these objects would reionize the universe by $z \gtrsim 20$ (Couchman & Rees 1986). Instead, in inhomogeneous reionization scenarios, widely separated but very luminous sources of photoionizing radiation such as QSOs, present at the time the IGM is largely neutral, will generate expanding H II regions whose size is only limited by the individual source lifetime. The universe will be divided into an ionized phase whose filling factor $q(z)$ increases with time, and an ever-shrinking neutral phase (Arons & Wingert 1972; Meiksin & Madau 1993). If the ionizing sources are randomly distributed, the H II regions will be spatially isolated for $q \ll 1$. The IGM will become completely reionized at the breakthrough epoch, when $q = 1$ and the IGM is fully transparent at the Lyman continuum. Current QSO counts suggest that the breakthrough epoch may occur as recently as $z \gtrsim 5$ (Meiksin & Madau 1993).

It is therefore of great interest, in testing rival reionization scenarios, to seek any evidence of nonuniformity in the ionization structure of the IGM by studying the thermal and ionization history of the intergalactic gas surrounding isolated sources of radiation (see, e.g., Miralda-Escudè & Rees 1994). In this paper we shall discuss how radioastronomical measurements of spectral and spatial structures in the 21 cm line emission and absorption from H I at high redshifts may provide a valuable tool for probing the epoch of the likely heat input at $5 \lesssim z \lesssim 10$ and its nature, e.g., whether it was limited to small isolated regions or was relatively diffuse. We will confine our analysis to epochs prior to complete reionization, and address the physical state of the gas that has not yet been engulfed by an ionized region.

For intergalactic H I to be observable in 21 cm line emission or absorption against the cosmic background radiation, the spin temperature must differ from the CBR temperature. As the former will in general be a weighted mean between the matter and CBR temperatures, an efficient mechanism for coupling the populations of the hyperfine levels to the kinetic state of the intergalactic gas is needed to unlock the spin state from the CBR. At the low particle densities characteristic of the IGM, the dominant coupling mechanism is level-mixing via Lyα photon scattering—the "Wouthuysen-Field" effect. We present in this paper a new heating mechanism, arising from atomic recoil in response to the scattering of resonant photons. We demonstrate that because of resonant scattering heating, Lyα coupling makes the detection of the IGM in absorption against the CBR quite unlikely, since the same Lyα photons that pump the hyperfine levels heat the atoms as well. This is not entirely surprising, as the energetic demand for raising the kinetic temperature above that of the CBR is relatively small, $\sim 10^{-7}$ eV cm^{-3} at $z \sim 7$, hence, even a relatively inefficient heating mechanism like Lyα resonant scattering may become important.

We find that the heating requirements are quite generally met in a variety of scenarios in which radiation sources turn on at high redshifts. We show that, in models based on QSO photoionization, and well before the H II region network has fully percolated, the (mostly) neutral IGM between the H II bubbles will be photoelectrically heated to temperatures above a few hundred degrees by soft X-ray photons from the QSOs. In CDM models a similar mechanism may efficiently warm the IGM at $z \lesssim 7$, since galactic mass halos with virial temperatures $\sim 10^6$ K are significant sources of thermal bremsstrahlung radiation. Alternatively, if protogalaxies at these early epochs are forming stars at a rate that is only $\sim 10\%$ of the global present-day star formation rate, heating by background Lyα "continuum" photons could drive the kinetic temperature of the still neutral material well above the radiation temperature of the microwave background. As a consequence, we conclude that *most of the neutral IGM will be available for detection at* 21 cm *only in emission.*

Two scenarios serve to illustrate the observability at meter wavelengths of the intergalactic medium during reionization. An isolated QSO turning on in a neutral medium will create an H II bubble surrounded by an X-ray warmed neutral zone. Sufficiently near the QSO, the spin state of the neutral IGM will be coupled to its kinetic state by redshifted continuum Lyα photons from the QSO. This zone will then emit 21 cm radiation that would be detectable against the CBR as a differential intensity, in angle or frequency. A stronger signal may be achieved in the presence of a Lyα continuum background sufficiently strong to couple the spin temperature of the cold and neutral IGM outside the QSO "sphere of influence" to the kinetic temperature of the IGM. The larger signal results from the enhanced contrast between the 21 cm absorbing medium far from the QSO, and the 21 cm emitting gas in the X-ray warmed neutral zone surrounding the QSO H II region. This phase, however, will be short-lived: through atomic recoil the Lyα background photons will soon heat the IGM far from the QSO to a temperature above that of the CBR, and absorption will cease.

The plan of the paper is as follows. In § 2 we discuss sources of radiation at high redshift. In § 3 we review the mechanisms that determine the level populations of the hyperfine state of neutral hydrogen. In § 4 we treat the preheating of the IGM prior to complete reionization and show that a 21 cm absorbing IGM can exist only as a transitory state. In § 5 we argue that the 21 cm line signature from a neutral IGM, redshifted to meter wavelengths, will appear as a small feature in the radio extragalactic background on scales of $\lesssim 1^\circ$ and may be detectable with the Giant Metrewave Radio Telescope. Finally, in § 6, we summarize our conclusions.

2. SOURCES OF RADIATION AT HIGH REDSHIFT

In the following, we assume that the universe is completely reionized by discrete sources at $z \gtrsim 5$, and that the IGM at such early epochs is uniform on large scales. Unless otherwise stated, we shall adopt a flat cosmology with $q_0 = 0.5$ and $H_0 = 50\, h_{50}$ km s^{-1} Mpc^{-1}.

2.1. *QSO* H II *Regions*

When an isolated point source of ionizing radiation turns on, the ionized volume initially grows in size at a rate fixed by the emission of UV photons, and an ionization front separating the ionized and neutral regions propagates into the neutral gas. The evolution of an expanding cosmo-

logical I front in a uniform IGM is governed by the equation

$$4\pi r_I^2 n_{\rm H}\left(\frac{dr_I}{dt} - Hr_I\right) = S - \frac{4}{3}\pi r_I^3(1+2\chi)n_{\rm H}^2\alpha_B \qquad (1)$$

(Shapiro 1986), where r_I is the proper radius of the I front, $n_{\rm H}$ is the hydrogen density of the IGM, H is the Hubble constant, S is the number of ionizing photons emitted by the central source per unit time, $\alpha_B \simeq 2.6 \times 10^{-13} T_4^{-0.845}$ cm^3 s^{-1} is the recombination coefficient to the excited states of hydrogen, and T_4 is the gas temperature in units of 10^4 K. A helium-to-hydrogen cosmic abundance ratio $\chi = 1/12$ is adopted, with both H and He fully ionized inside the H II region. The right-hand side of equation (1) is a measure of the net flux of ionizing photons reaching the I front after subtracting recombinations and vanishes at the Strömgren radius, $r_{\rm St} = \{3S/[4\pi n_{\rm H}^2\alpha_B(1+\chi)]\}^{1/3}$. Across the I front the degree of ionization changes sharply on a distance of the order of the mean free path of an ionizing photon. Denoting by $\Omega_{\rm IGM}$ the baryonic mass density parameter of the intergalactic medium, the I front will expand at the speed of light for

$$r_I < \left(\frac{S}{4\pi n_{\rm H} c}\right)^{1/2} \approx (2.85\ {\rm Mpc})\left(\frac{S}{10^{57}\ {\rm s}^{-1}}\right)^{1/2} \times \left(\frac{\Omega_{\rm IGM}h_{50}^2}{0.05}\right)^{-1/2}\left(\frac{1+z}{7}\right)^{-3/2}, \qquad (2)$$

to subsequently slow down because of geometrical dilution. In an expanding IGM, the ionization front generated by a QSO, with $S \sim 10^{57}$ s^{-1}, or a star forming galaxy, with $S \sim 10^{53}$ s^{-1}, will fail to grow to even half of its Strömgren radius (Shapiro 1986; Madau & Meiksin 1991). In this case radiative recombinations within the H II region may be neglected on the right-hand side of equation (1) (proportional to $r_{\rm St}^3 - r_I^3$), to obtain at a short time after the turn-on epoch z (corresponding to the redshift interval $\Delta z \ll 1+z$),

$$r_I \approx (10.2\ {\rm Mpc})\left(\frac{S}{10^{57}\ {\rm s}^{-1}}\right)^{1/3} h_{50}^{-1/3}\left(\frac{\Omega_{\rm IGM}h_{50}^2}{0.05}\right)^{-1/3} \times \left(\frac{1+z}{7}\right)^{-11/6}\Delta z^{1/3}, \qquad (3)$$

and

$$v_I \approx (2.2 \times 10^4\ {\rm km\ s}^{-1})\left(\frac{S}{10^{57}\ {\rm s}^{-1}}\right)^{1/3} h_{50}^{2/3} \times \left(\frac{\Omega_{\rm IGM}h_{50}^2}{0.05}\right)^{-1/3}\left(\frac{1+z}{7}\right)^{2/3}\Delta z^{-2/3}. \qquad (4)$$

For comparison, the radius of the light front around each source is

$$r_c \equiv c\,\Delta t \approx (46.3\ {\rm Mpc})h_{50}^{-1}\left(\frac{1+z}{7}\right)^{-5/2}\Delta z. \qquad (5)$$

2.2. *Virialized Halos*

In CDM dominated cosmologies, galactic mass halos will begin to collapse at high redshift ($z > 5$). The hot gas in these halos will produce a soft X-ray background radiation field via thermal bremsstrahlung. We estimate the number of halos using the Press-Schechter formalism (Press & Schechter 1974), which should suffice for an order of magnitude estimate for systems on these scales.

The (proper) volume emissivity per unit frequency due to thermal bremsstrahlung radiation from isothermal, optically thin halos is

$$\epsilon_{\rm halo}(\nu) = (3.2 \times 10^{36}\ {\rm ergs\ Mpc^{-3}\ s^{-1}\ Hz^{-1}}) \times \int_0^\infty dr_0\, N(r_0, z)(1+z)^3 n_{\rm halo}^2(r_0)\frac{4\pi}{3}r_v^3 T(r_0)^{-1/2} \times \exp\left[-\frac{h\nu}{kT(r_0)}\right], \qquad (6)$$

where $N(r_0, z)$ is the number of halos per unit comoving volume per initial comoving size r_0 at redshift z, $n_{\rm halo}(r_0)$ is the internal hydrogen density of a halo, and $T(r_0)$ is its temperature. The hydrogen is assumed to be shock heated to the virial temperature and collisionally ionized. In spherical top-hat collapse, the temperature T and radius r_v of a virialized halo are related to r_0 by $kT(r_0) = 1.4\mu m_{\rm H}(1+z_c)H_0^2 r_0^2$ and $r_0 = 5.6(1+z_c)r_v$, where z_c is the collapse redshift of the perturbation, and $\mu \approx 0.6$ is the mean molecular weight of a fully ionized gas of cosmic abundances. The internal density of the cloud exceeds the external density at the projected time of collapse by a factor of 178. Normalizing to a baryon density of $\Omega_{\rm IGM}h_{50}^2 = 0.05$ gives $n_{\rm halo} = 1.8 \times 10^{-5}(1+z_c)^3$ cm^{-3}. According to the Press-Schechter formalism,

$$N(r_0, z)dr_0 = -3\frac{1.686(1+z)}{(2\pi)^{3/2}r_0^4\Delta(r_0)}\frac{d\log\Delta(r_0)}{d\log(r_0)} \times \exp\left[-\frac{1.686^2(1+z)^2}{2\Delta(r_0)^2}\right]dr_0. \qquad (7)$$

Here, $\Delta(r_0)$ is the rms mass fluctuation in a sphere of radius r_0. We will adopt a pure CDM spectrum for a $q_0 = 0.5$, $H_0 = 50$ km s^{-1} Mpc^{-1} universe (Bardeen et al. 1986). This model appears to provide an adequate representation of the power spectrum on small scales when appropriately renormalized, even though a higher normalization is needed for an optimal match to the temperature fluctuations measured by *COBE* on large scales (Górski et al. 1995). Normalizing to the abundance of clusters, Δ (16 Mpc) ≈ 0.6 (White, Efstathiou, & Frenk 1993), we find that for $0.2 < r_0 < 1$ Mpc, $\Delta(r_0) \approx 3.6 r_0^{-3/8}$, where r_0 is measured in megaparsecs.

The total emissivity above a minimum photon energy $h\nu_{\rm min}$ is $\epsilon_{\rm halo} = [kT(r_0)/h]\epsilon_{\rm halo}(\nu_{\rm min})$, after integrating equation (6) over frequency. While the emissivity from an individual halo increases for increasing temperature (for $kT < h\nu_{\rm min}$), the number of halos decreases rapidly. At any given redshift, the peak contribution to the integral in equation (6) arises, therefore, from some intermediate size halo. We may thus approximate this integral by performing a second-order Taylor expansion of the exponent about the halo size. Most of the bremsstrahlung radiation is found to be emitted by halos with an initial comoving radius

$$\hat{r}_0 \approx (1\ {\rm Mpc})\left(\frac{h\nu_{\rm min}}{20\ {\rm ryd}}\right)^{4/11}\left(\frac{1+z}{7}\right)^{-12/11}. \qquad (8)$$

The total emissivity is given by

$$\epsilon_{\rm halo} \approx (2.6 \times 10^{43}\ {\rm ergs\ Mpc^{-3}\ s^{-1}})\hat{r}_0^{3/8} \times \left(\frac{1+z}{7}\right)^7 \left[\frac{kT(\hat{r}_0)}{20\ {\rm ryd}}\right] \left(\frac{h\nu_{\rm min}}{20\ {\rm ryd}}\right)^{-1/2} \times \exp\left[-5.3\left(\frac{1+z}{7}\right)^2 \hat{r}_0^{3/4} - 1.8 \times \left(\frac{1+z}{7}\right)^{-1} \left(\frac{h\nu_{\rm min}}{20\ {\rm ryd}}\right) \hat{r}_0^{-2}\right]. \quad (9)$$

We shall use this expression in § 4.2.3 below to estimate the virialized halo contribution to the heating rate of the IGM.

2.3. *Early Stellar Populations*

An early generation of stars may provide a background radiation field of Lyα photons that arises from the collective redshifted continua of the stars. The background specific intensity associated with a constant comoving emissivity from the present epoch to redshift $z_{\rm max}$, as seen by an observer at redshift z, is given by

$$J_\alpha(z) = \frac{1}{4\pi}\,\epsilon(\nu_\alpha, 0)(1+z)^{3+\alpha_S} \int_z^{z_{\rm max}} \frac{dl}{dz'}\,(1+z')^{-\alpha_S}\,dz', \quad (10)$$

where $\epsilon(\nu_\alpha, 0)$ is the Lyα volume emissivity due to stars in galaxies at the present epoch, dl/dz' is the proper differential line element in a Friedmann cosmology, and we have assumed a power-law energy spectrum. Here, $1 + z_{\rm max} \approx 4(1+z)/3$, as photons emitted at higher redshifts will have wavelength below 912 Å at the source and will be strongly attenuated by Lyman-continuum intergalactic absorption. Weakly dependent on α_S, equation (10) may be rewritten as

$$J_\alpha(z) \approx (10^{-20.7}\ {\rm erg\ cm^{-2}\ s^{-1}\ Hz^{-1}\ sr^{-1}}) h_{50}^{-1} \times \left[\frac{\epsilon(\nu_\alpha, 0)}{10^{25}\ {\rm ergs\ Mpc^{-3}\ s^{-1}\ Hz^{-1}}}\right] \left(\frac{1+z}{7}\right)^{3/2}. \quad (11)$$

Using the results of the Hα survey of Gallego et al. (1995), we estimate the continuum emissivity from present day galaxies at the frequency of Lyα to be, to within a factor of 2, $\epsilon(\nu_\alpha, 0) \approx 4 \times 10^{25}$ ergs Mpc^{-3} s^{-1} Hz^{-1}. Only a fraction of this emissivity would be available at high redshift from dwarf galaxies or the progenitors of today's bright galaxies. The Lyα continuum emissivity at early epochs, however, may be even larger if pregalactic Population III stars are present at these times.

The IGM will still be mostly neutral if the background intensity at the Lyman edge, J_L, satisfies

$$J_L < \frac{hc}{4\pi}\,n_{\rm H}(0)(1+z)^3 \approx (10^{-21.2}\ {\rm erg\ cm^{-2}\ s^{-1}\ Hz^{-1}\ sr^{-1}}) \times \left(\frac{\Omega_{\rm IGM} h_{50}^2}{0.05}\right)\left(\frac{1+z}{7}\right)^3, \quad (12)$$

i.e., if less than one ionizing photon per hydrogen atom has reached the IGM by that epoch. Because the integrated UV spectrum of a stellar population is characterized by a strong Lyman-continuum break (about a factor of 4), and, more importantly, only a small fraction of ionizing photons might escape from collapsed star forming regions into intergalactic space (see Madau & Shull 1996), one expects $J_L \ll J_\alpha$. Hence, based on a comparison of equations (11) and (12), it is plausible to assume a largely neutral medium even in the presence of a significant Lyα background from an early generation of stars, $J_{\alpha,-21} \approx 1$.

3. SPIN TEMPERATURE OF THE INTERGALACTIC MEDIUM

The amount of emission or absorption from a neutral intergalactic medium is determined by the spin state of the atoms. The spin temperature may be coupled to the matter both through the scattering of Lyα photons—the Wouthuysen-Field effect (Wouthuysen 1952; Field 1958)—and atomic collisions. At the low particle densities characteristic of intergalactic gas, and in the presence of radio-quiet radiation sources, the dominant coupling mechanism is Lyα scattering.

3.1. *Lyα Radiation Color Temperature*

The Wouthuysen-Field effect mixes the hyperfine levels of neutral hydrogen via the intermediate step of transitions to the $2p$ state. According to this mechanism, an atom initially in the $n = 1\ {}_0S_{1/2}$ singlet state may absorb a Lyα photon that will put it in the $n = 2\ {}_1P_{1/2}$ or ${}_1P_{3/2}$ state, allowing it to return to the triplet $n = 1\ {}_1S_{1/2}$ state by spontaneous decay. Similarly, a triplet atom may absorb a slightly lower frequency photon to reach the same upper state, followed by decay to the singlet state. The efficiency of the effect is determined by the frequency dependence of the background radiation field J_ν near Lyα. In particular, the excitation rates of the hyperfine levels depend on the relative intensities of the blue and the red wings of Lyα. To observe the 21 cm line in absorption or emission, the excitation and deexcitation rates of the hyperfine levels must be comparable to or exceed those due to 21 cm continuum background radiation.

The Lyα line absorption cross section is

$$\sigma_\nu = \sigma_\alpha\,\phi(\nu) = \frac{\pi e^2}{m_e c}\,f_\alpha\,\phi(\nu) = \frac{3}{8\pi}\,\lambda_\alpha^2 A_\alpha\,\phi(\nu) \quad (13)$$

(neglecting the very small correction due to stimulated emission, of order $\lambda_\alpha^3 J_\alpha/2hc \ll 1$), where A_α and f_α are the spontaneous Einstein coefficient and upward oscillator strength for the transition, $\phi(\nu)$ is the line profile function [with normalization $\int \phi(\nu)d\nu = 1$], and all other symbols have their usual meanings. The absorption rate of Lyα photons is proportional to $B_{jk}\int d\nu\phi(\nu)J_\nu$, where B_{jk} is the Einstein stimulated absorption coefficient from level j to level k, where we now mean to include the hyperfine structure of the atom. [The coefficients are related to the total spontaneous decay rates A_{kj} between the various hyperfine levels by $B_{jk} = (\lambda_{jk}^3/8\pi h)(g_k/g_j)A_{kj}$.] When the intensity varies smoothly across the H I absorption profile for Lyα, that is, over at least one Doppler width $\Delta\nu_{\rm D} = (b/c)\nu_\alpha$, where $b = (2kT_K/m_{\rm H})^{1/2}$ and ν_α is the line center frequency, it is useful to express the effect of the mixing mechanism in terms of the color temperature T_α of the radiation field, which we define by

$$\frac{1}{kT_\alpha} = -\frac{\partial \log \mathcal{N}_\nu}{\partial h\nu}, \quad (14)$$

evaluated at $\nu = \nu_\alpha$, where $\mathcal{N}(\nu)$ is the photon occupation number at frequency ν, $\mathcal{N}(\nu) = c^2 J_\nu/(2h\nu^3)$. If the background continuum spectrum near Lyα is a power law, $J_\nu \propto \nu^{-\alpha_S}$, then $T_\alpha = (h\nu_\alpha/k)/(3+\alpha_S) \approx 3 \times 10^4$ K$[4/(3+\alpha_S)]$. It has been shown by Field (1959b), however, that, because of the large cross section for resonant scattering, the shape of

the radiation spectrum near Lyα will be determined in all the relevant physical situations by the kinetic temperature of the scattering material. This tendency for thermalization is caused by the recoil of the atom, which shifts the profile to the red. As stimulated emission is negligible, the radiation behaves like a classical relativistic Boltzmann gas, and the specific number density of photons, $n_\nu = 4\pi J_\nu/ch\nu$, assumes the quasi-LTE form $n_\nu = \text{const} \times \exp[-h(\nu - \nu_\alpha)/kT_K]$, where T_K is the kinetic temperature of the gas, to which the color temperature relaxes.

The influence of cosmological expansion on the Lyα profile has been discussed by Field (1959a). The effect of expansion is determined by two timescales, the mean free scattering time for a Lyα photon, $b/(cn_{\rm H\,I}\sigma_\alpha\lambda_\alpha)$, where $n_{\rm H\,I}$ is the density of neutral hydrogen, and the time it takes the Hubble expansion to redshift a photon through the resonance, $b/(Hc)$. Their ratio, also known within the framework of line radiation transfer theory as the Sobolev parameter (and equal in this context to the inverse of the Lyα optical depth), is

$$\gamma \equiv \frac{H}{\lambda_\alpha \sigma_\alpha n_{\rm H\,I}} \approx 6 \times 10^{-6} h_{50} \left(\frac{1+z}{7}\right)^{-3/2} \left(\frac{\Omega_{\rm IGM} h_{50}^2}{0.05}\right)^{-1} . \tag{15}$$

As this is much smaller than unity, the Lyα part of the radiation background spectrum establishes close thermal contact with the expanding IGM, and a quasi-static treatment of the cosmological line transfer is an adequate approximation (see, e.g., Rybicki & Dell'Antonio 1994). The profile of Lyα radiation in an expanding cloud has been calculated in detail by Deguchi & Watson (1985). These authors consider the case in which Lyα photons are created by recombinations inside the cloud. They show that $T_\alpha \to T_K$ for $\gamma \lesssim 10^{-5}$, similar to what is found in the absence of velocity gradients (Field 1959b). The color temperature approaches the gas kinetic temperature even more quickly if the cloud is irradiated by continuum radiation in the vicinity of Lyα, as this spectrum is already flat in frequency, and only a small number of scatterings is needed for the radiation field to achieve the proper slope (Deguchi & Watson 1985). In the next section we shall see how, in the presence of a strong ambient flux of Lyα photons, the color temperature governs the hyperfine populations of atomic hydrogen.

3.2. *Lyα Photon Pumping*

In the absence of collisions, the spin temperature, T_S, of the hyperfine levels of intergalactic hydrogen (as defined by the Boltzmann equation) is determined solely by the scattering of ambient Lyα photons and by the microwave background radiation field at 21 cm (Field 1958, 1959a).[2] In a steady state we have

$$T_S = \frac{T_{\rm CBR} + y_\alpha T_\alpha}{1 + y_\alpha} , \tag{16}$$

where $T_{\rm CBR} = 2.73(1+z)$ K is the temperature of the cosmic background radiation (Mather et al. 1994), and

$$y_\alpha \equiv \frac{P_{10}}{A_{10}} \frac{T_*}{T_\alpha} \tag{17}$$

is the normalized probability, or Lyα pumping "efficiency." Here, $T_* \equiv h\nu_{10}/k = 0.07$ K, $A_{10} = 2.9 \times 10^{-15}$ s^{-1} is the spontaneous decay rate of the hyperfine transition of atomic hydrogen, P_{10} is the indirect de-excitation rate of the triplet via absorption of a Lyα photon to the $n = 2$ level, and we have assumed $T_S \gg T_*$. In the absence of Lyα pumping the spin temperature goes to equilibrium with the 21 cm background radiation field on a timescale $T_*/(T_{\rm CBR} A_{10}) \approx 5 \times 10^4$ yr, and neutral intergalactic hydrogen cannot be seen in either 21 cm emission or absorption. If y_α is large, $T_S \to T_\alpha \approx T_K$, signifying equilibrium with the matter. The $1 \to 0$ transition rate via Lyα can be replaced by the total rate P_α,

$$P_\alpha = \int d\Omega \int \frac{I_\nu}{h\nu} \sigma_\nu \, d\nu , \tag{18}$$

at which Lyα photons are scattered by an H atom in the gas, $P_{10} = 4P_\alpha/27$. For a point source, $I_\nu = f_\nu \delta(\Omega)$, where f_ν is the specific flux from the source. For an isotropic radiation field, $I_\nu = J_\nu$. In the limit $T_\alpha \gg T_{\rm CBR}$, the fractional deviation in a steady state of the spin temperature from the temperature of the microwave background is

$$\frac{T_S - T_{\rm CBR}}{T_S} \approx \left[1 + \frac{T}{y_\alpha T_\alpha}\right]^{-1} . \tag{19}$$

There exists then a critical value of P_α which, if much exceeded, would drive $T_S \to T_\alpha$. This "thermalization rate" is found to be

$$P_{\rm th} \equiv \frac{27 A_{10} T_{\rm CBR}}{4 T_*} \approx (5.3 \times 10^{-12} \text{ s}^{-1}) \left(\frac{1+z}{7}\right) . \tag{20}$$

When $P_\alpha = P_{\rm th}$, we have $T_S = 2T_{\rm CBR}/(1 + T_{\rm CBR}/T_\alpha)$. It should be emphasized that, while T_α depends on the spectral gradient across line center, $y_\alpha T_\alpha$, and hence $P_{\rm th}$, are only functions of the magnitude of J_α, independent of the uncertainties regarding the actual profile of the Lyα background photon spectrum.

3.3. *Level Mixing by Lyα Continuum Photons*

There are four possible sources of background Lyα photons propagating into the (mostly) neutral material that has not yet been engulfed by an H II region: (1) UV, nonionizing continuum emitted by the radiating sources and then redshifted by the Hubble expansion to the Lyα wavelength in the absorbing medium rest frame; (2) Lyα photons generated by radiative recombinations and escaping from the H II regions; (3) Lyα produced locally in the warm neutral material surrounding the ionized gas by radiative recombinations; and (4) by collisional excitations. Of these, only the first, continuum photons redshifted into local Lyα, is a significant source of coupling, and we treat it next. We show that the remaining three are generally negligible in Appendix A.

In the limit where the scattering occurs close to the emission redshift, we find for a point source

$$P_\alpha \approx (2.3 \times 10^{-10} \text{ s}^{-1}) r_{\rm Mpc}^{-2} L_{\alpha,47} , \tag{21}$$

where $L_{\alpha,47}$ is the source Lyα luminosity per octave in photon energy in units of 10^{47} ergs s^{-1}, and $r_{\rm Mpc}$ is the (physical) distance in Mpc between emission and scattering. Thus, within several Mpc from a bright, radio-quiet QSO, $P_\alpha > P_{\rm th}$ and the spin temperature of neutral hydrogen will

[2] This is not strictly true in the presence of bright continuum sources of 21 cm radiation such as radio-loud quasars (see § 3.5.).

be determined by the Lyα continuum photons emitted from the quasar itself.

Alternatively, we may consider the effect of an integrated intensity from a distribution of sources. The Lyα scattering rate is then

$$P_\alpha \approx (8.5 \times 10^{-12}\ \mathrm{s}^{-1}) J_{\alpha,-21}\ , \tag{22}$$

where $J_{\alpha,-21}$ is the intensity of the background diffuse field at Lyα in units of 10^{-21} ergs cm^{-2} s^{-1} Hz^{-1} sr^{-1}. For $J_{\alpha,-21} \ll 1$, the spin system will go into equilibrium with the microwave background. Equation (22) is also approximately valid in the case of recombination Lyα photons, as radiative transfer calculations predict $dJ_\nu/d\nu = 0$ at the Doppler core of the transition (Urbaniak & Wolfe 1981). Spectral gradients induced by atomic recoil only result in higher order corrections for P_α. The rate is therefore dependent only on J_α.

The Lyα pumping mechanism poses a difficulty for detecting the IGM in absorption against the CBR, since, as we will show below, the same Lyα photons that mix the hyperfine levels of hydrogen heat the atoms as well. Before we discuss this problem, we briefly address the influence of particle collisions and direct radio continuum on the spin temperature.

3.4. *Hyperfine Excitation via Particle Collisions*

We demonstrate in this section that, except at very high redshifts, or in overdense regions, collisions are not effective in coupling the spin temperature to the kinetic temperature. One can show that, in the general case, the spin temperature may be written in the form (Field 1958)

$$T_S = \frac{T_{\mathrm{CBR}} + y_\alpha T_\alpha + y_c T_K}{1 + y_\alpha + y_c}\ , \tag{23}$$

where

$$y_c \equiv \frac{C_{10}}{A_{10}} \frac{T_*}{T_K}\ , \tag{24}$$

and C_{10} is the rate of collisional de-excitation of the triplet level (see eqs. [16] and [17]). Emission occurs for

$$\frac{y_\alpha T_\alpha + y_c T_K}{y_\alpha + y_c} \approx T_K > T_{\mathrm{CBR}}\ , \tag{25}$$

and absorption otherwise. Unless the electron density is larger than a few percent of the hydrogen density, the collisional de-excitation rate is dominated by collisions with other hydrogen atoms through spin exchange (Purcell & Field 1956). Allison & Dalgarno (1969) give a maximum de-excitation rate of $C_{10}/n_{\mathrm{H}} = 3.3 \times 10^{-10}$ cm^3 s^{-1} for $T_K < 1000$ K, with a value a factor of 2.6 lower at $T_K = 100$ K. To couple the spin temperature to the kinetic temperature requires a collision rate $C_{10} > A_{10} T_{\mathrm{CBR}}/T_*$, or a density $n_{\mathrm{H}} > 3 \times 10^{-4}(1+z)$ cm^{-3}. This may occur only for $1 + z > 55(\Omega_{\mathrm{IGM}} h_{50}^2/0.05)^{-1/2}$. At $z \sim 6$, collisions will mix the hyperfine levels if $\delta\rho/\rho \gtrsim 100$, i.e., in the case of nearly virialized halos.

3.5. *Radio-loud Quasars*

So far, we have limited our attention to radio-quiet sources of radiation. However, 21 cm radiation emitted by quasi-stellar radio sources could raise the spin temperature of neighboring intergalactic H I above the CBR temperature (Bahcall & Ekers 1969; Urbaniak & Wolfe 1981). At a distance r from the QSO, the brightness temperature at 21 cm is

$$T_R = \frac{c^2}{8\pi k \nu_{10}^2} \frac{L_\nu}{4\pi r^2}\ , \tag{26}$$

where L_ν is the absolute luminosity of the radio-emitting QSO at 1.4 GHz. The typical radio quasar power is a small fraction of the B-band luminosity,

$$(\nu L_\nu)_{5\ \mathrm{GHz}} \approx 4 \times 10^{-4} (\nu L_\nu)_B \tag{27}$$

(e.g., Phinney 1985). So, assuming νL_ν is roughly constant in the radio, we derive

$$T_R \approx (30\ \mathrm{K}) \left[\frac{(\nu L_\nu)_B}{10^{47}\ \mathrm{ergs\ s^{-1}}}\right] r_{\mathrm{Mpc}}^{-2}\ . \tag{28}$$

This temperature must be added to T_{CBR} in equation (16) for determining the level populations. Comparison with equation (21), however, shows that in the presence of UV photons this term is very small compared to the Lyα pumping term and so can safely be neglected.

4. PREHEATING OF THE INTERGALACTIC MEDIUM

While a cold IGM may be detected in absorption against the CBR, when the spin and kinetic temperatures are coupled through the Wouthuysen-Field mechanism, the period for which absorption is possible is short-lived. The reason is that the Lyα photons that couple the spin and kinetic temperatures will quickly heat the IGM through atomic recoil to a temperature above that of the CBR. In this section, we return to the radiation sources introduced in § 2 and discuss their roles as heating sources by Lyα scattering and by photoelectric heating by soft X-rays.

4.1. *Lyα Heating*

The effect of recoil due to the finite mass of the atom was first discussed in resonance-line scattering by Field (1959b) (see also Adams 1971; Basko 1981). Contrary to the case of radiation scattered by free electrons (where a systematic shift in frequency due to recoil can produce large cumulative effects), in problems of resonance-line transfer a photon on the red side of the line has a heavy bias toward scattering back to the blue. This bias suppresses the additive effect of recoil: because of Doppler redistribution, a photon largely loses memory of its injection energy, and the background intensity develops only a slight asymmetry in frequency at line center (matching the slope of the Planck function in the Wien limit, see Field 1959b) even at the large Lyα optical depths normally encountered in astrophysical situations. However, it is through the recoil of the atom that the radiation field exchanges energy with the gas in scattering problems. In this section we shall discuss in some detail the effect of repeated Lyα resonant scattering on the thermal state of a cold, neutral IGM. A more formal derivation of the rate of transfer of energy from the radiation field to the atoms is provided in Appendix B.

The average relative change in a Lyα photon's energy E after having been scattered by a hydrogen atom at rest is

$$\left\langle \frac{\Delta E}{E} \right\rangle = -\frac{h\nu_\alpha}{m_{\mathrm{H}} c^2} \approx -10^{-8}\ , \tag{29}$$

where $m_{\rm H}$ is the mass of the hydrogen atom. It should be noted that this is an approximation valid only for $h\nu_\alpha \gg kT_K$. In the opposite limit, energy will flow from the atoms to the photons. Through recoil, energy is transferred from photons to atoms at a rate

$$\dot{E}_\alpha = -\left\langle \frac{\Delta E}{E} \right\rangle h\nu_\alpha P_\alpha \,. \tag{30}$$

where P_α is the Lyα scattering rate per H atom. In the case of excitation at the thermalization rate $P_{\rm th}$, equation (30) becomes

$$\dot{E}_{\rm th} = \frac{27}{4}\frac{(h\nu_\alpha)^2}{m_{\rm H}c^2}\frac{A_{10}\,T_{\rm CBR}}{T_*} \approx (220\ {\rm K\ Gyr^{-1}})\left(\frac{1+z}{7}\right). \tag{31}$$

This rate is sufficient to drive the intergalactic gas kinetic temperature above the temperature of the cosmic background radiation in a fraction $\approx 15\%$ *of the Hubble time at* $z = 6$. As a consequence, a low-density IGM is observable in absorption at 21 cm for only a brief interval of time once coupling is established. In general, coupling through the Wouthuysen-Field mechanism leads to emission.

This may be illustrated for the case of an early population of stars. It follows from equations (11) and (22) that the equivalent of only $\sim 10\%$ of the global present-day star formation rate is required for P_α to exceed $P_{\rm th}$, and so drive $T_S \rightarrow T_K$. The IGM would initially be observed in absorption, but after $\sim 10^8$ yr the IGM will be heated to a temperature above $T_{\rm CBR}$ by resonant scattering of the Lyα photons.

It is of interest to compare Lyα heating with heating by X-ray photons. The amount of energy deposited via photoionization by soft X-rays is, allowing for secondary ionizations, a few tens of eV per photon. There are also a few free electrons for every photon, as recombinations are negligible. In contrast, the total energy available for Lyα heating (whether the Lyα photon is part of the continuum or due to recombinations) is, neglecting the energy lost to cosmological expansion, given by the photon energy multiplied by the fractional line width. This is typically 0.001 eV photon^{-1}. Therefore, at least of order one Lyα photon per atom is needed to raise the kinetic temperature of the IGM above $T_{\rm CBR}$. If we denote by $L_{\rm X}$ the soft X-ray luminosity of a young galaxy (associated with, e.g., supernova remnants, X-ray binaries, etc.), then photoelectric heating will dominate over Lyα heating if $L_{\rm X}/L_\alpha \gtrsim 10^{-4}$. As the typical observed value for L^* galaxies is $L_{\rm X}/L_\alpha \sim 10^{-2}$ (e.g., Fabbiano 1989; Bennett et al. 1994), Lyα photons from galaxies are an inefficient heating source compared to X-rays.[3]

4.2. *Soft X-Ray Heating*

4.2.1. *Heating Rate by Quasars*

It is widely believed that the integrated ultraviolet flux arising from QSOs and/or hot, massive stars in metal-producing young galaxies is responsible for maintaining the intergalactic diffuse gas and the Lyα forest clouds in a highly ionized state at $z \lesssim 5$. In this and the next section we shall focus on a reionization scenario dominated by hard-spectrum quasar sources. In this case, while the radiation just shortward of the hydrogen Lyman edge will be absorbed at the ionization front generated by an individual QSO, very short wavelength photons will be able to propagate to much greater distances, $r_c > r_I$. The intensity of the QSO radiation flux at the light front will be reduced by the opacity of the (mostly) neutral gas surrounding the expanding H II region,

$$\tau_\nu = n_{\rm H\,I}(r_c - r_I)(\sigma_\nu^{\rm H\,I} + \chi\sigma_\nu^{\rm He\,I})\,, \tag{32}$$

where $\sigma_\nu^{\rm H\,I}$ and $\sigma_\nu^{\rm He\,I}$ are the hydrogen and helium photoionization cross sections. For $\Omega_{\rm IGM}h_{50}^2 = 0.05$, $z > 5$, and $r_c - r_I = 10$ Mpc, the photoelectric optical depth will drop below unity for photon energies above 16 ryd. Thus, most of the photoelectric heating of the IGM will be accomplished by soft X-rays. The heating by such high-energy photons, however, is not as efficient as for photons near the photoelectric threshold because of losses to collisional excitation of H I and He I and to the collisional production of secondary electrons (Spitzer & Scott 1969). The fraction f of photon energy converted into heat is then a sensitive function of the H II fraction. At the light front, this fraction is the residual ionization left over from the recombination epoch. For $h_{50} = 1$ and $\Omega_{\rm IGM} = 0.05$, this is $\sim 5 \times 10^{-4}$ (Peebles 1993, chap. 6), which gives $f \approx 0.17$ (Shull & van Steenberg 1985). For a quasar with a spectral index α_S shortward of 1 ryd, the heating rate per hydrogen atom at the light front is given by

$$\dot{E}_X(r_c) = \alpha_S \frac{S}{4\pi r_c^2}\, h\nu_L f \times \int_1^\infty dx x^{-1-\alpha_S}[\sigma_\nu^{\rm H\,I}(x-1) + \chi\sigma_\nu^{\rm He\,I}(x-1.8)]e^{-\tau_\nu}\,, \tag{33}$$

where $x \equiv \nu/\nu_L$, and ν_L is the frequency at the H I Lyman edge. Both the H I and He I photoelectric cross sections scale approximately as ν^{-3} far from threshold. In this approximation the integral becomes exact and may be expressed as

$$\dot{E}_X(r_c) \approx \left[(1400\ {\rm K\ Gyr^{-1}})\alpha_S\,\Gamma\left(\frac{2+\alpha_S}{3}\right)\tau_*^{(1-\alpha_S)/3}\right] \times \left(\frac{f}{0.17}\right)\left(\frac{S}{10^{57}\ {\rm s^{-1}}}\right)\left(\frac{\Omega_{\rm IGM}h_{50}^2}{0.05}\right)^{-(2+\alpha_S)/3} \times \left(\frac{1+z}{7}\right)^{-2-\alpha_S}\left(1-\frac{r_I}{r_c}\right)^{-(2+\alpha_S)/3} \times \left(\frac{r_c}{25\ {\rm Mpc}}\right)^{-(8+\alpha_S)/3}, \tag{34}$$

where $\Gamma(x)$ is the usual gamma function. Here, τ_* normalizes the opacity of the IGM for soft X-ray frequencies according to $\tau_\nu = \tau_*(\Omega_{\rm IGM}h_{50}^2/0.05)[(1+z)/7]^3(r_c/25\ {\rm Mpc})(1 - r_I/r_c)(\nu/\nu_L)^{-3}$. Numerically, $\tau_* \approx 7.8 \times 10^4$. For $\alpha_S = 1.5$, the coefficient in square brackets is ~ 300 K Gyr^{-1}. The heating rate is dominated by helium absorption, which exceeds the hydrogen contribution by $\sim 2{:}1$. The intergalactic gas at the light front will be heated to a temperature above that of the cosmic background radiation in a fraction

[3] As shown by Rees (1985), the radiation pressure associated with trapped Lyα background photons is also unlikely to affect the condensing out of overdense regions of the IGM even in the linear regime.

of the Hubble time,

$$\frac{\Delta t_{\rm heat}}{t_H} \approx \left[0.02\,\frac{\tau_*^{(\alpha_S-1)/3}}{\alpha_S\,\Gamma\{(2+\alpha_S)/3\}}\right] h_{50}\left(\frac{f}{0.17}\right)^{-1} \times \left(\frac{S}{10^{57}\ {\rm s}^{-1}}\right)^{-1}\left(\frac{\Omega_{\rm IGM}h_{50}^2}{0.05}\right)^{(2+\alpha_S)/3}\left(\frac{1+z}{7}\right)^{9/2+\alpha_S} \times \left(1-\frac{r_I}{r_c}\right)^{(2+\alpha_S)/3}\left(\frac{r_c}{25\ {\rm Mpc}}\right)^{(8+\alpha_S)/3}. \quad (35)$$

For $\alpha_S = 1.5$, the coefficient in square brackets is ~ 0.1. The H II region produced by a QSO will therefore be preceded by a warming front. Heating by soft X-rays is so efficient that the size of the warm zone will extend nearly to the light front. Note that, as the X-ray–heated bubbles around QSOs will survive as fossils even after the quasar has died, several generations N_g of quasars may actually be responsible for preheating the entire IGM. For a typical QSO age of $t_Q \approx 3 \times 10^8 N_g^{-1/3}$ yr, the required QSO comoving space density to heat the entire IGM to a temperature above that of the CBR by $z \approx 6$ is $\sim 10^{-10}$ Mpc$^{-3} N_g^{-1}$. By comparison, the comoving space density of bright QSOs at $z = 4$ is $\sim 100 N_g$ times larger (Warren, Hewett, & Osmer 1994). Note that, if all bright galaxies undergo a quasar phase, QSOs must have a very short lifetime, and $N_g \sim 100$. Soft X-rays from a few bright QSO sources could then prevent collapsing structures, such as protoclusters while still in the linear regime, from being detected in 21 cm absorption against the CBR (Scott & Rees 1990).

4.2.2. *Numerical Solution for Expanding Warm* H I *Regions around Quasars*

We illustrate the thermal effect of an expanding H II region on the surrounding medium by numerically solving the time-dependent equations for photoionization and heating around a point source that turns on suddenly in a homogeneous, expanding universe. We have integrated as a function of time the ionization equations for hydrogen and helium, including photoionization, collisional ionization, and radiative recombination, on a radial grid with a local ionization flux equal to $L_\nu \exp(-\tau_\nu)/4\pi r^2$, where τ_ν is given by equation (32). The flux is set to zero beyond the light front to prevent unphysical excess heating at large distances. We use the time-dependent ionization algorithm of Meiksin (1994) and include here the generation of secondary electrons by soft X-rays. We adopt the fitting formulas of Shull & van Steenberg (1985) to include the additional ionization and energy losses associated with the production of these electrons. We solve the time-dependent energy equation along with the ionization equations for a gas of primordial hydrogen and helium composition, including photoelectric heating and radiative losses due to collisional excitation and ionization, radiative recombination, Compton cooling off the CBR, and cooling by expansion. An accurate numerical solution for the growth of the H II region requires grid zones that are optically thin to the ionizing radiation when the hydrogen is still fully neutral. Thicker zones are ionized too rapidly, resulting in a too rapidly growing I front. Because we wish to follow the heating out to the light radius, however, this restriction imposes a prohibitive demand on our computing resources. The demand imposed by helium ionization is less restrictive because of its lower density and so may be met. We therefore adopt a compromise. A grid sufficiently fine to resolve the helium ionization is used, but it is somewhat too coarse to follow the evolution of the H II I front accurately. To prevent too rapid a growth of the H II front, we set the flux to zero for energies less than 1.8 ryd, the He I ionization potential. We find this results in accurate placement of the H II front, though the details of its structure may not be quite correct. Because helium ionization and the soft X-ray heating are governed by the opacity outside the H II front, this approach yields an accurate solution for the He II and He III fronts and the external heating rate in the surrounding neutral IGM.

In Figure 1, we show the results of an integration for a QSO turning on at $z = 6$ with a gradual rise over a time of 10^7 yr to a peak photoionizing luminosity of $S = 10^{57}$ s^{-1}, and with $\alpha_S = 1.5$, in a medium with $\Omega_{\rm IGM}h_{50}^2 = 0.05$. By $z = 5.5$, the QSO has heated the surrounding gas to a temperature exceeding that of the CBR to a (proper) distance of 23 Mpc, compared to the light front radius of 25 Mpc. The temperature climbs inward, reaching 1000 K at a distance of 10 Mpc from the QSO. The ionization fronts are at 7.5 Mpc at this time. Neither the He II nor the He III fronts extend much beyond that of hydrogen, but for different reasons. Because of the much higher photon energy required to photoionize He II compared to H I, the radius of the He III front can exceed that of H II by at most a factor of $(4^{-\alpha_S}/\chi)^{1/3} \simeq 1.1$, despite the low helium abundance (see Madau & Meiksin 1994). While the energy needed to photoionize He I

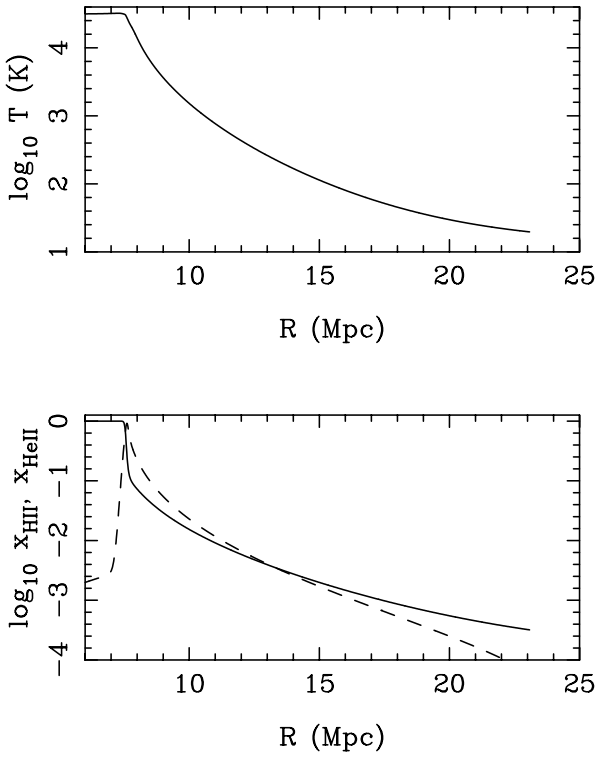

FIG. 1.—Numerical calculation of the IGM surrounding a QSO (assumes $q_0 = 0.5$, $H_0 = 50$ km s^{-1} Mpc^{-1}, $\Omega_{\rm IGM} = 0.05$). The QSO was turned on gradually at $z = 6$ with a specific luminosity of $L_\nu = 10^{31}$ ergs s^{-1} Hz^{-1} $(\nu/\nu_L)^{-1.5}$. The effects of secondary electrons are significant for soft X-rays, and have been included, along with radiative cooling mechanisms and Compton cooling of the CBR. (*top*) Temperature of the IGM due to soft X-ray heating by the QSO. At $z = 5.5$, the IGM is heated to a temperature above that of the cosmic background radiation out to a radius of 23 Mpc. The light front is at 25 Mpc. (*bottom*) H II (*solid line*) and He II (*dashed line*) fractions. The ionized region surrounding the QSO extends to 7.5 Mpc at this time.

is smaller, the IGM is more optically thick at the lower energy. At $z = 5.5$, the opacity of H I at the He I edge reaches unity a distance 10 kpc beyond the H II ionization front. Outside the H II region, H I efficiently shields the helium from the ionizing radiation above 1.8 ryd, ensuring that it remains mostly neutral. The He I is then able to warm through the absorption of the incident soft X-rays emitted by the QSO.

4.2.3. *Heating Rate by Virialized Halos*

Galactic mass halos provide another source of heating in CDM-dominated cosmologies. While before stars form the numbers of these halos are small, too small to account for the ionization of the IGM by UV photons, we demonstrate here that a sufficient number of halos will collapse to provide the soft X-rays required to heat the IGM to a temperature above that of the cosmic background radiation.

We start with equation (9), which gives the background emissivity above a minimum photon energy. To specify its value, we observe that, at sufficiently low energies, the distance a photon travels before being absorbed in the IGM will be shorter than the mean separation of the sources, so that only part of the IGM will be penetrated by such photons. We set the minimum energy according to the criterion that the filling factor of photons with energy above $h\nu_{\rm min}$ be greater than unity. For $5 < z < 10$, this yields

$$h\nu_{\rm min} \approx 15.2 \text{ ryd} \left(\frac{1+z}{7}\right)^{3/2}, \tag{36}$$

corresponding to a halo of comoving size $\approx$0.9 Mpc, virial temperature $\approx 1.5 \times 10^6$ K, and total mass $\approx 2 \times 10^{11} M_\odot$. Approximated in this manner, the emissivity is only half of the value given in equation (9), since halos with $r_0 < \hat{r}_0$ are excluded by the filling factor criterion. Note that the collisional ionization level of helium in such hot halos is so large that absorption of soft X-rays within the halos themselves is completely negligible. Substituting equation (36) into equation (9), and taking into account the factor of 2, we find for the heating rate of the halos per hydrogen atom

$$\dot{E}_X^{\rm halo} \approx (2.6 \times 10^5 \text{ K Gyr}^{-1}) \left(\frac{f}{0.2}\right) \left(\frac{1+z}{7}\right)^3 \times \exp\left[-6.6\left(\frac{1+z}{7}\right)^{1.6}\right], \tag{37}$$

where $f \approx 0.2$ accounts for the energy loss to collisional excitations and ionizations per incident X-ray photon (Shull & van Steenberg 1985), for an assumed H II fraction of 10^{-3}. We show the heating rate in Figure 2. The IGM will be heated to a temperature above that of the CBR in a fraction of the Hubble time,

$$\frac{\Delta t_{\rm heat}^{\rm halo}}{t_H} \approx (7.5 \times 10^{-5}) \left(\frac{f}{0.2}\right)^{-1} \left(\frac{1+z}{7}\right)^{-0.5} \times \exp\left[6.6\left(\frac{1+z}{7}\right)^{1.6}\right]. \tag{38}$$

At $z = 6$, this fraction is 0.05. Because the merging of small halos into larger ones is an ongoing process, the full Hubble time will not be available to the halos at any given stage in the hierarchy for heating the IGM. Moreover, the halos will

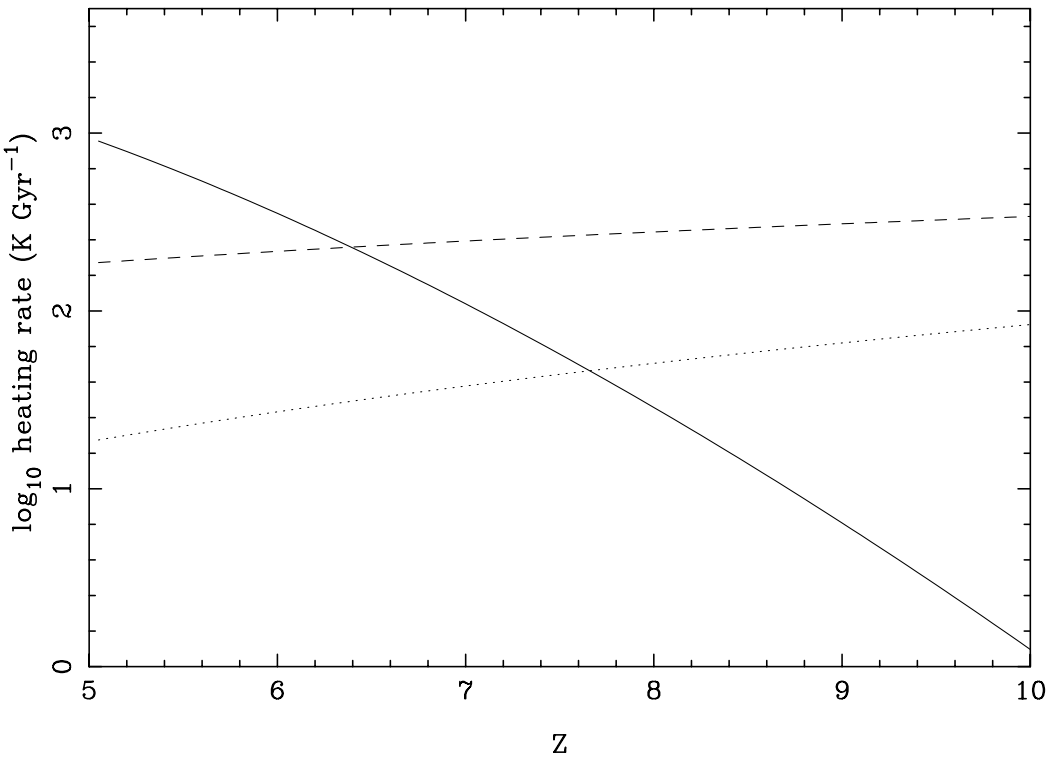

FIG. 2.—Heating rate per hydrogen atom of the IGM due to soft X-rays from collapsed galaxy halos, in a flat $q_0 = 0.5$ and $H_0 = 50$ km s^{-1} Mpc^{-1} CDM-dominated cosmology (*solid line*). Also shown is the required heat input over a Hubble time to match the CBR temperature, $1.5T_{\rm CBR}(z)/H(z)$ (*dotted line*). For $z < 7$, the rate of X-ray heating from collapsed halos is sufficient to raise the temperature of the IGM above that of the CBR. At higher redshifts, the IGM is too dense and the hot halos that can produce the required penetrating soft X-rays are too few for efficient heating. At these epochs, only part of the IGM will be heated above the CBR temperature. The heating rate $\dot{E}_{\rm th}$ due to Lyα resonant scattering (*dashed line*) is shown for a background radiation field sufficiently strong to couple the spin temperature to the kinetic temperature of the IGM (see text).

cool by radiative processes on a timescale of $t_{\rm cool}/t_H \simeq 0.7[(1+z)/7]^{-3/2} T_6^{1.8}$ (Gould & Thakur 1970), and even more quickly at high redshifts by Compton cooling off the CBR. The cooling, however, may not be significant for $z < 10$ before the gas is reheated by mergers in the next stage of the hierarchy. Allowing the halos to provide X-ray photons for 50% of the Hubble time, they will heat the IGM to a temperature of ~ 100 K by $z = 6$. At higher redshifts, halo heating may still be important in overdense environments like protoclusters where the number density of halos may be substantially boosted by statistical bias (Bardeen et al. 1986). Of course once stars start to form, they, or more likely their remnants, may dominate the soft X-ray emission of an individual halo. In this sense, the halo emissivity calculations outlined above present a lower limit to the heating rate of the IGM at early epochs.

It is worth noting that, while the X-rays are an efficient heating mechanism of the gas, they are an inefficient source of photoionization. This is because the time required to photoionize the IGM by X-ray photons is larger by a factor of $\sim (15 \text{ ryd}/kT_{\rm CBR}) \approx 10^5$, since now it is the number of ionizing photons rather than their energy that counts. The ionization time thus exceeds the Hubble time by a few orders of magnitude, and the IGM will remain mostly neutral.

4.2.4. *Thermal Coupling between Neutral Atoms and Ions*

In the discussion above, we have assumed that the energy deposited by the photons is strongly coupled to the hydrogen. The thermal energy, however, is initially contained in the photoejected electrons and ions only. In this section we shall verify that the equilibration mechanisms between the various ions and neutrals in the low-density IGM are sufficiently rapid to ensure that all species are thermally coupled.

We first consider Coulomb coupling between the ions. The time for two different species i and j to reach thermal equilibrium through Coulomb scattering is

$$t_{\rm eq}(i,j) \approx (5.87 \text{ s}) \frac{A_i A_j}{(n_i + n_j) Z_i^2 Z_j^2 \log \Lambda} \left(\frac{T_i}{A_i} + \frac{T_j}{A_j} \right)^{3/2}, \quad (39)$$

(Spitzer 1962). Each species has a temperature T, density n, charge Z, and molecular weight A ($A = 1/1836$ for electrons). (This expression applies strictly only when the total energy between the two species, $n_i T_i + n_j T_j$, is conserved during the equilibration process. For a single species, $j = i$ may be set in eq. [39] if the coefficient 5.87 is replaced by 8.06.) In the physical regime of interest, $20 < \log \Lambda < 50$. Once the electrons and protons each reach equilibrium separately (the shortest two timescales), the bottleneck for all the ions to relax to a single temperature is proton-electron scattering, with a coupling time

$$t_{\rm eq}(e,p) \approx (3.3 \text{ Myr}) \left(\frac{x_e}{10^{-3}} \right)^{-1} \left(\frac{1+z}{7} \right)^{-3} \times \left(\frac{\Omega_{\rm IGM} h_{50}^2}{0.05} \right)^{-1} T_4^{3/2}, \quad (40)$$

where x_e is the number of electrons per hydrogen nucleus. After these two species equilibrate, singly and doubly ionized helium follow shortly through proton scatters. Note that, as the postphotoionization (by 16 ryd soft X-rays) temperature of electrons is $\sim 10^6$ K, the time for protons to thermalize with such high-energy electrons by Coulomb collisions alone actually exceeds the Hubble time. At these energies, however, the primary photoelectrons will quickly cool via the production of secondary electrons by the collisional ionization and excitation of neutral hydrogen (Spitzer & Scott 1969). The cooling rates of an electron of energy E ryd by these two processes are comparable and are given by

$$t_{\rm cool} \approx (0.03 \text{ Myr}) \left(\frac{1+z}{7} \right)^{-3} \left(\frac{\Omega_{\rm IGM} h_{50}^2}{0.05} \right)^{-1} \frac{E^{3/2}}{\log E} \quad (41)$$

(Shull & van Steenberg 1985). For $E = 16$, this gives $t_{\rm cool} \approx 0.6$ Myr. The result is an energy distribution of primary and secondary electrons that declines sharply above the Lyα excitation energy of 10.2 eV (Bergeron & Souffrin 1971).

The coupling rate is still small for electrons of these energies, but they further lose energy through elastic scattering off neutral hydrogen atoms. The electron-hydrogen cross section for a 10 eV electron is about $7\pi a_0^2$, where a_0 is a Bohr radius (Moiseiwitsch 1962). The corresponding relaxation timescale is

$$t_{\rm eq}(e, \text{H}) \approx (25 \text{ Myr}) \left(\frac{1+z}{7} \right)^{-3} \left(\frac{\Omega_{\rm IGM} h_{50}^2}{0.05} \right)^{-1}. \quad (42)$$

The electrons can finally cool to temperatures below $\sim 10^4$ K. Once a thermal distribution of electrons has been established, new energetic electrons generated by X-ray photoionization will reach equipartition with the cooler electrons on a much shorter timescale by Coulomb losses (Shull & van Steenberg 1985).

The distance from the light front for which the temperature of the neutral hydrogen atoms lags behind the electron temperature corresponding to equation (42) is ~ 8 Mpc. This, however, assumes complete thermalization. The less stringent requirement that the neutral hydrogen atoms be heated to a temperature large compared to the cosmic background radiation temperature will be satisfied on a somewhat shorter timescale. The number of QSOs required to heat the IGM above the cosmic background radiation temperature may then exceed the estimate given in § 4.2.1 by a factor of a few only.

The neutrals will reach a single common temperature relatively quickly. The interaction between neutral hydrogen atoms is dominated by elastic scattering.[4] The equilibration time is $t_{\rm eq} = 2/n_{\rm H\,I} \langle u\sigma \rangle$, where $\langle u\sigma \rangle$ is the slowing down coefficient for hydrogen atom collisions (Spitzer 1978). Using the elastic collision cross section from Allison & Smith (1971), this gives

$$t_{\rm eq}(\text{H}, \text{H}) \approx (0.4 \text{ Myr}) \left(\frac{1+z}{7} \right)^{-3} \left(\frac{\Omega_{\rm IGM} h_{50}^2}{0.05} \right)^{-1} T_4^{-1/4}. \quad (43)$$

Thus, all the species will reach a common temperature within a timescale much shorter than the Hubble time, and it is safe to assume that the hydrogen atoms may be described by a single Maxwellian energy distribution.

5. OBSERVATIONS OF REDSHIFTED 21 CENTIMETER LINE RADIATION

In this section we discuss how radio measurements may reveal 21 cm line radiation from a neutral IGM at high redshift. The Giant Metrewave Radio Telescope (GMRT),

[4] Provided that statistical equilibrium has been established between the singlet and triplet ground state levels. This is achieved on a timescale $\sim 5 \times 10^4$ yr by collisions with CBR photons.

scheduled for completion by 1997, has two frequency bands that are best suitable for detecting 21 cm radiation at $z > 5$, viz., 150 ± 20 and 235 ± 8 MHz (Swarup 1996). The central frequencies of these bands correspond to $z = 8.5$ and 5.0, respectively. Because of its high sensitivity for both compact and extended sources, the GMRT will be a valuable instrument for cosmological studies in the redshift ranges $4.85 < z < 5.25$ and $7.35 < z < 9.9$. We focus the discussion on measurements in the 150 MHz band, corresponding to $z \approx 8$.

We have assumed that the IGM at early epochs is uniform on large scales. One general issue is the effect of small-scale clumping. In a CDM-dominated cosmology, inhomogeneity on subgalactic scales develops before the first quasars form (if the latter require galactic-mass collapsed structures). This may delay the eventual percolation of H II regions and increases the value of J needed to balance recombinations and to maintain full ionization. It is unlikely that clumping would change the present discussion by very much. It leaves unchanged the amount of heating and ionization due to each UV photon, as well as the rate at which the heating and ionization fronts advance around a quasar. Even in an overdense region (unless the overdensity is extreme), recombinations are unimportant over the lifetime of a single quasar (or during the time it takes for the heating front to advance). It is also worth emphasizing that there will unavoidably be nonuniformities in the 21 cm intensity due to density inhomogeneities, but that these are restricted to smaller scales than those due to the patchy heat input (at least in the QSO case). While we confine our discussion to larger scales, it would nonetheless be worthwhile to consider means for their detection.

To illustrate the basic principle of the observations we propose, consider a region of neutral material with spin temperature $T_S \neq T_{\rm CBR}$, having angular size on the sky that is large compared to a beam width, and radial velocity extent due to the Hubble expansion, which is larger than the bandwidth. Its intergalactic optical depth at $21(1 + z)$ cm along the line of sight,

$$\tau(z) = \frac{3c^3h^3n_{\rm H\,I}(0)A_{10}}{32\pi H_0 k^3 T_*^2 T_S}(1+z)^{1.5} \approx 10^{-2.9}h_{50}^{-1} \times \left(\frac{T_{\rm CBR}}{T_S}\right)\left(\frac{\Omega_{\rm IGM}h_{50}^2}{0.05}\right)(1+z)^{1/2}, \quad (44)$$

will typically be much less than unity. The experiment envisaged consists of two measurements, separated in either angle or frequency, such that one measurement, the fiducial, detects no line feature, either because there is no H I or because $T_S \approx T_{\rm CBR}$, and the second at $T_S \neq T_{\rm CBR}$. As the brightness temperature through the IGM is $T_b = T_{\rm CBR}\,e^{-\tau} + T_S(1 - e^{-\tau})$, the differential antenna temperature (which is the relevant quantity since we are considering a detector operating as a comparison system), observed at Earth between this region and the CBR will be

$$\delta T = (1+z)^{-1}(T_S - T_{\rm CBR})(1 - e^{-\tau}) \approx (0.011\ {\rm K})h_{50}^{-1}\left(\frac{\Omega_{\rm IGM}h_{50}^2}{0.05}\right)\left(\frac{1+z}{9}\right)^{1/2}\eta, \quad (45)$$

where we have defined a "21 cm radiation efficiency" as

$$\eta \equiv x_{\rm H\,I}\left(\frac{T_S - T_{\rm CBR}}{T_S}\right). \quad (46)$$

Here $x_{\rm H\,I}$ refers to the neutral fraction of the hydrogen in the region for which $T_S \neq T_{\rm CBR}$. As long as T_S is much larger than $T_{\rm CBR}$ (hence, if there has been significant preheating of the intergalactic gas), $\eta \to x_{\rm H\,I}$, and the IGM can be observed in emission at a level independent of the exact value of T_S. By contrast, when $T_{\rm CBR} \gg T_S$ (negligible preheating), the differential antenna temperature appears, in absorption, a factor $\sim T_{\rm CBR}/T_S$ larger than in emission and it becomes relatively easier to detect intergalactic neutral hydrogen (Scott & Rees 1990). Note that in a universe with $q_0 \ll \frac{1}{2}$, δT increases more nearly linearly with $(1 + z)$, and the numerical coefficient in equation (45) may be larger by up to a factor $3[(1 + z)/9]^{1/2}$. Depending on the cosmology, δT will increase toward low frequencies at a rate between $\nu^{-1/2}$ and ν^{-1}.

The discrete nature of the sources of preheating and 21 cm excitation will cause δT to have a distinctive structure both in frequency and in angle across the sky, as will be shown below. It is important to point out that the radio signal from the IGM will be swamped by the much stronger nonthermal background that dominates the radio sky at meter wavelengths. This synchrotron-type component has brightness temperature

$$T_b(z=0) \approx 6\ {\rm K}\left(\frac{\lambda}{1\ {\rm m}}\right)^{2.8}, \quad (47)$$

which is consistent with the integrated contribution from discrete radio sources (see Longair 1995 for a recent review). The anisotropic galactic contribution is about 3 times larger. Such emission will cause intensity fluctuations from beam to beam, either from discrete radio sources or from variable galactic brightness. Hence, the difficulty is to be able to discriminate between the IGM around a QSO with a brightness temperature of 0.01 K against a small fluctuation in the galactic and extragalactic background. Clearly, to remove this foreground contamination, some differential mapping technique must be used. The line radiation from high-z gas might, e.g., be distinguished against continuum emitting sources owing to its sharp and distinctive spectral feature, i.e., by making measurements at two frequencies sufficiently close that the continuum emission from discrete sources does not vary significantly (Bebbington 1986).

In the following sections we will illustrate by a few examples the sensitivity of the detailed pattern of sky brightness at redshifted 21 cm wavelengths to the unknown thermal and ionization history of the universe.

5.1. *Quasars in a Background of UV Radiation at $z \approx 8$*

In the theories for the origin of cosmic structure that are most popular today, massive objects grow by hierarchical clustering—low-mass perturbations collapse early, then merge into progressively larger systems. In such a scenario, one naturally expects the high-redshift universe to contain small-scale substructures, systems with virial temperature well below 10^4 K. The resultant virialized systems will remain as neutral gas clouds unless they can cool due to molecular hydrogen, in which case they may form Population III stars. These stars will then ionize the gas in their vicinity. It is less clear, however, whether or not a sufficient number of ionizing photons will be able to penetrate all of the surrounding neutral gas in the cloud to reach the external intergalactic gas and ionize it. Nonetheless, the stars will still produce a background of UV continuum photons near the Lyα frequency that can escape.

It is therefore of interest to consider a case in which QSOs turn on in a universe where the Lyα scattering rate is $P_\alpha \approx P_{\rm th}$ everywhere, i.e., where

$$J_\alpha = J_{\rm th} \equiv \frac{9}{2}\frac{A_{10}\nu_\alpha^3}{A_\alpha \nu_{10}}\frac{kT_{\rm CBR}}{c^2} \approx (10^{-21.1}\ {\rm erg\ cm^{-2}\ s^{-1}\ Hz^{-1}\ sr^{-1}})\left(\frac{1+z}{9}\right), \quad (48)$$

(see eqs. [20] and [22]). The Lyα photons will propagate into uncollapsed regions of the IGM, where the kinetic temperature in the absence of heating will be

$$T_K(z) \approx 0.026\ {\rm K}(1+z)^2 \quad (49)$$

(Couchman 1985), well below $T_{\rm CBR}$ because of adiabatic cooling during cosmic expansion. The Lyα flux will couple the spin temperature to the kinetic temperature, and T_S will be pulled below $T_{\rm CBR}$. (Note that, in the absence of a radiative coupling agent like Lyα, this could only happen in very high baryon density models, where collisions would remain important even at modest redshifts, Scott & Rees 1990.)

As shown in § 4.1, however, the same Lyα photons that mix the hyperfine levels will also heat the gas through recoil. Integrating the energy equation, assuming the Lyα field is turned on, or more precisely reaches the level of equation (48), at redshift z_α, and using equations (31) and (49), we find

$$T_K(z) \approx (0.026\ {\rm K})(1+z)^2 + (160\ {\rm K})(1+z)^2 \times [(1+z)^{-5/2} - (1+z_\alpha)^{-5/2}]\ . \quad (50)$$

The characteristic timescale for heating the medium above the CBR temperature via Lyα resonant scattering at the thermalization rate is

$$\Delta t_{\rm heat} = \frac{2}{9}\frac{m_{\rm H}c^2\nu_{10}}{h\nu_\alpha^2}A_{10}^{-1} \approx 10^8\ {\rm yr}\ , \quad (51)$$

about 20% of the Hubble time at $z \approx 8$. The heating rate corresponding to equation (48) is shown in Figure 2. The result is a finite interval of time during which Lyα photons couple the spin temperature to the kinetic temperature of the IGM before heating the IGM above the CBR temperature. If Lyα sources turned on at redshifts $z_\alpha \lesssim 10$, this interval would present a window of opportunity in redshift space near $z \approx 8$ that would enable a large fraction of intergalactic gas to be observable at $\sim$160 MHz in *absorption* against the CBR.

In such a scenario, 21 cm emission on tens of megaparsecs scale would still be produced by the relatively rare, X-ray heated regions associated with QSO sources. If we denote by $T_{S,w}$ the spin temperature of the "warm" ($T_{S,w} \gg T_{\rm CBR}$) gas, and by $T_{S,c}$ the spin temperature of the surrounding, more pervasive "cold" ($T_{S,c} < T_{\rm CBR}$) medium, as given by equation (50), the differential antenna temperature observed between these two phases of the IGM will be proportional to the effective efficiency

$$\Delta\eta = T_{\rm CBR}\left(\frac{x_{\rm H\,I,c}}{T_{S,c}} - \frac{x_{\rm H\,I,w}}{T_{S,w}}\right). \quad (52)$$

Here, we distinguish between the neutral fractions in the cold and warm regions, to allow the warm zone to refer either to the inside or the outside of the ionized bubble. Even though the H I in the cold region is absorbing the CBR, by using the flux through the cold gas as a fiducial, the signature of the cold gas will appear as *emission* from the warm regions surrounding the quasars. The effective efficiency will remain much larger than unity, $\Delta\eta \approx T_{\rm CBR}/T_{S,c} \gtrsim 4$, only for $\lesssim 10^7$ yr (see eq. [50]), to drop to $\Delta\eta \approx 2$ after $\approx 5 \times 10^7$ yr. Note that $\Delta\eta \approx 4$ corresponds to temperature fluctuations of about 0.04 K. This flux is well below the level of the Bebbington's (1986) radio survey, but would be reachable with an instrument like the GMRT in several hours of integration.

For illustrative purposes, consider now the sphere of influence associated with a quasar ($L_{\alpha,47} = 1$, $\alpha_S = 1.5$) that turned on at $z = 8.7$, nearly synchronized with a Lyα background of sources turned on at $z = 9$, and radiating isotropically. At $z = 8$, e.g., after 5×10^7 yr the QSO will have ionized a bubble of size $r_I \approx 7.5$ Mpc and heated the surrounding H I within $r_c \approx 15$ Mpc. In Figure 3*a* we show $\Delta\eta$ as a function of radius at various epochs, including the effect of Lyα heating on the cold phase. The peak value at the I front initially exceeds unity, but declines as $T_{S,c}$ rises. The quasar has created a shell of 21 cm emission surrounding the H II region with a thickness of $\Delta r \approx 7.5$ Mpc. The hydrogen column density through the shell's width is $\approx 2 \times 10^{21}$ cm^{-2}, and its total H I mass is $\approx 2 \times 10^{16}\ M_\odot$. The angular size on the sky corresponding to the diameter of the emitting region is

$$2\theta = \frac{H_0(1+z)^2 r_c}{c(1+z-\sqrt{1+z})} \approx 2^\circ\ . \quad (53)$$

The shell will have a characteristic radial double peaked profile, as the gas in its interior will be completely ionized, as shown in Figure 3*b*. The velocity difference across each peak, due to the Hubble flow, is $\Delta v = H_0(1+z)^{3/2}\Delta r \approx$ 10,000 km s^{-1}. Between the inner edges of the two peaks, Δv is twice as large, since $\Delta r \approx r_I$ at this time. At 150 MHz, we would then observe two signals (the front and back of the shell) with flux density

$$\delta S \approx (6\ {\rm mJy})h_{50}^{-1}\left(\frac{\Omega_{\rm IGM}h_{50}^2}{0.05}\right)\left(\frac{1+z}{9}\right)^{-3/2}\left(\frac{\Delta\eta}{2.2}\right) \quad (54)$$

(see eqs. [45] and [52]), extending over and separated by about 5 MHz, nearly the entire bandwidth of the receiver. For a fixed velocity width, δS increases linearly with the mass of the shell.

Let us analyze in some detail the detectability of a typical 21 cm emitting shell with the GMRT. The 30 antennas of the GMRT will be configured as a Y of 16 dishes with a central compact core of 14 dishes. Because the GMRT functions as an interferometer, it is insensitive to angular scales exceeding $\sim\lambda/d$, where d is the separation of the dishes. If we wish to measure $\sim 2^\circ$ scale structures at 150 MHz ($\lambda \sim 2$ m), the projected separation of antennas is required to be about $d \lesssim 50$ m. Since the GMRT antennas have a diameter of about 45 m, the GMRT interferometric system will not be sensitive to 2° scale structures as the antennas will start shadowing each other for projected spacings less than 45 m.

An alternative strategy is to measure the total power by incoherent addition of the outputs of the 30 GMRT antennas, for which the effective collecting area will be 30×0.5 that of one antenna. For observations at 150 MHz the theoretical rms thermal noise of the GMRT output in incoherent mode is ≈ 1 mJy for the following parameters: T(sys) $\sim$ 600 K, A(eff) $\sim$ 1000 m^2 for one 45 m dish, a band-

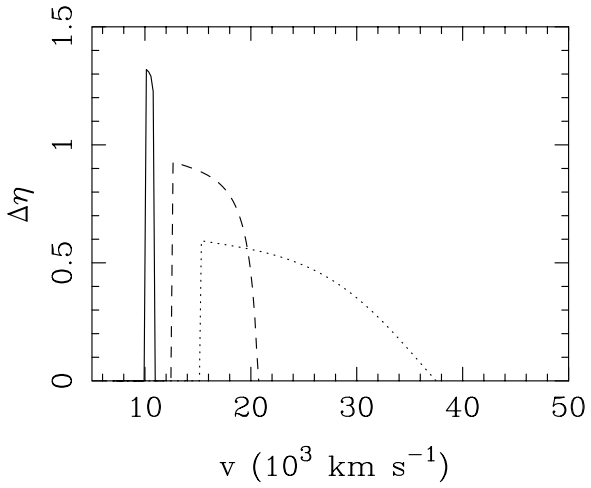

FIG. 3a

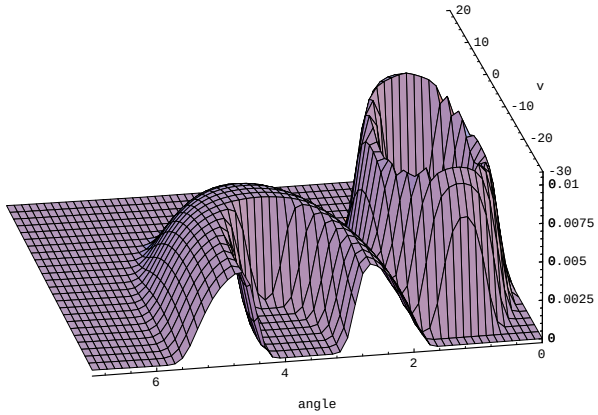

FIG. 3b

FIG. 3.—(*a*) 21 cm efficiency is shown as a function of distance from a QSO with $L_{\alpha,47} = 1$ and $\alpha_S = 1.5$, turning on at $z = 8.7$. A Lyα radiation field of intensity $J_{\alpha,-21} = 0.8[(1+z)/9]$ was turned on at $z = 9$ and partially couples the spin temperature of the neutral hydrogen to the kinetic temperature. The effect of heating of the IGM by Lyα collisions is included. The efficiency is shown at time intervals of 2.5, 5, and 10×10^7 yr after QSO turn-on, corresponding to $z = 8.3$, 8.0, and 7.4, respectively. Because the IGM temperature is less than that of the cosmic background radiation at early times, a large efficiency is achieved in an X-ray warmed shell surrounding the quasar. (*b*) Map of the differential antenna temperature (K) as a function of angle (deg) and velocity shift (10^3 km s^{-1}) (differenced from 21 cm redshifted to 153 MHz), resulting from two quasars turning on at $z = 8.7$, as in (*a*). One quasar is at a comoving position corresponding to $z = 7.4$ and the other at $z = 8.0$. The quasars are separated by 2°.5 on the sky. Such a map could be constructed by making a sequence of angular maps in a given frequency band, here taken to be 2000 km s^{-1} wide, and stepping in frequency until the full emitting region surrounding the quasars is recovered. In practice, a bandwidth of 5000–10,000 km s^{-1} will give a more feasible integration time for establishing a positive detection. The emission is measured relative to a reference beam well-separated from the quasars, either by frequency or by angle.

width of 10,000 km s^{-1} (5 MHz), and 5 hr integration for each of the two frequency bands separated by about 5 MHz (Swarup & Malik 1996). A comparison with equation (54) shows that ~ 100 hr of integration will be required to detect an individual shell at 5 $\sigma_{\rm rms}$. This time is comparable to that proposed for searches for emission from collapsing H I clouds at high redshift (Swarup et al. 1991; Subramanian & Padmanabhan 1993; Swarup 1996). However, it is not clear whether the above sensitivity can be realized in practice because of the man-made noise and variations of the instrumental gain and the galactic background temperature over two bands separated by 5 MHz. Note that, although the differential antenna temperature will be larger at earlier epochs because of the larger brightness contrast (i.e., less time to raise the temperature of the cold phase), the smaller radius of the QSO sphere of influence more than cancels the increase in emission efficiency. The signal-to-noise ratio improves slightly with increasing bubble size.

To calculate the expected number of emitting shells in a radio survey, we may estimate their effective covering factor on the sky as

$$C = \frac{c}{H} n_{\rm QSO} d_A^2 (\theta + \Theta)^2 \frac{\Delta v}{c} , \tag{55}$$

where $n_{\rm QSO}$ is the (proper) number density of quasars, d_A is the angular diameter distance, Θ is the field of view of the radio antenna (about 3°.1 at 150 MHz), and Δv measures the radial dimension covered by the survey. If the latter matches the shell thickness Δr, e.g., for a bandwidth of 5 MHz, the covering factor may be rewritten as

$$C = q_{21}\left(1 + \frac{\Theta}{\theta}\right)^2 \frac{\Delta r}{r_c} , \tag{56}$$

where q_{21} is the volume filling factor of the 21 cm emitting bubbles. As $\Theta^2 \Delta r/\theta^2 r_c \approx 5$, it follows from equation (56) that a shell will be detected after scanning about 20 fields with the GMRT if the filling factor of warm bubbles is $\approx 1\%$.

5.2. *Isolated Quasars*

We shall now analyze the model problem of an individual, isolated QSO turning on at epoch $z > 5$ in an otherwise unperturbed IGM. In this case the only radiative coupling agent is the continuum UV radiation of the quasar itself, redshifted to Lyα. From equations (21) and (20), it is useful to define a "thermalization distance" from a QSO, denoted by $r_{\rm th}$, at which $P_\alpha = P_{\rm th}$. Numerically, this yields

$$r_{\rm th} \approx (6\ {\rm Mpc})\left(\frac{1+z}{9}\right)^{-1/2} L_{\alpha,47}^{1/2} . \tag{57}$$

For the best case of $T_\alpha \gg T_{\rm CBR}$, the efficiency for 21 cm emission may be expressed, using equations (17), (19), (20), and (46), as $\eta = (1 + r^2/r_{\rm th}^2)^{-1}$. At $r = r_{\rm th}$, $\eta = \frac{1}{2}$. Comparison with equation (3) shows that the thermalization distance is comparable to the size of the H II region. Since $r > r_I$ is required for detection, $\eta > \frac{1}{2}$ may be achieved only for a brief redshift interval after the quasar turns on. This interval is so small for many quasars that their H II regions will still be in the luminal expansion stage (see eq. [2]), so that they will not be preceded by a warming front and will thus not be visible in 21 cm emission. The efficiency will therefore generally lie in the range $0 < \eta < \frac{1}{2}$.

Larger shells offer a slight advantage for detectability. This is because the flux of a shell emitting 21 cm radiation depends not only on its efficiency but on its size as well. The frequency integrated flux is proportional to

$$(\Omega\, \Delta v)_{\rm eff} \equiv 2\pi \int dv \int d\theta\theta\eta . \tag{58}$$

Consider a measurement made at a frequency corresponding to a depth in the emitting zone around the quasar just outside the I front, and with a bandwidth Δv_c matched to

the light radius r_c. Denoting by $\theta_{\rm th}$ the angle on the sky subtended by $r_{\rm th}$, integrating equation (58) out to r_c, using the expression above for η, gives $(\Omega\,\Delta\nu)_{\rm eff} \simeq 2\pi\theta_{\rm th}^2\,\Delta\nu_c[1 - (r_{\rm th}/r_c)\arctan(r_c/r_{\rm th})]$, when $r_c \gg r_I$. While the signal increases initially like the cube of the size of the emitting region, it does so only linearly at later times. Since the noise increases like $r_c^{3/2}$, the signal-to-noise ratio increases asymptotically only like $r_c^{1/2}$. Allowing for a light radius that subtends an angle θ_c on the sky of 1°, the flux is then

$$\delta S \approx (1\text{–}2\ \text{mJy}) h_{50} \left(\frac{\Omega_{\rm IGM} h_{50}^2}{0.05}\right)\left(\frac{1+z}{9}\right)^{-1/2} L_{\alpha,47} \quad (59)$$

over a bandwidth of $\Delta\nu_c \approx 11\ \text{MHz}[(1+z)/9]^{-1/2}(\theta_c/1°)$, comparable to the rms noise. It would thus take a few hundred hours of integration time on the GMRT to detect the shell at 5 $\sigma_{\rm rms}$. A quicker strategy may be to search for an excess variance across the sky over the rms noise that these shells would produce in the observed flux per resolution (beam width × bandwidth) element. A next generation facility like the Square Kilometer Array Interferometer (Braun 1996) could easily map warm IGM bubbles, effectively opening much of the universe to a direct study of the reheating epoch.

6. SUMMARY

The spectral appearance at 21 cm of nonuniform gas at high z had been previously investigated by Hogan & Rees (1979) and Scott & Rees (1990). These earlier papers showed that the 21 cm emission from high-z H I may display angular structure, as well as structure in redshift space; radio observations could therefore in principle yield "tomographic" mapping of protoclusters or other large-scale inhomogeneities at high redshifts, where the gas had not yet been reionized. The present work discusses how similar techniques may be used to reveal "patchiness" in the 21 cm emission due to nonuniformities in the spin temperature, rather than in the density. Such effects could tell us how (as well as when) the primordial gas was reheated; if the reheating were due to ultraluminous but sparsely distributed sources (e.g., the first QSOs), the resultant patches would have a larger scale than any gravitationally induced inhomogeneities, and would therefore be less difficult to detect. The continuum radiation, redshifted to Lyα, from an early generation of stars would couple the spin temperature to the low temperature of the IGM for a transitory interval before heating the gas above the CBR temperature. The result is a "window of opportunity" during which it may be possible to detect the IGM in absorption against the CBR, and in so doing possibly reveal the first epoch of star formation.

We have assessed three preheating mechanisms at early times: soft X-ray radiation from quasar sources, soft X-rays from virialized 10^{10}–10^{11} $M_\odot$ halos, and resonant scattering of background Lyα continuum photons from an early generation of stars, and argued that radiation sources at high redshifts may prevent collapsing structures that cannot cool efficiently from being detected in 21 cm absorption against the microwave background. We have shown that scattering of Lyα continuum radiation can mix the hyperfine levels of intergalactic H I within $\sim$10 Mpc of an individual QSO, and that this will produce an appreciable 21 cm emissivity from the IGM in the quasar neighborhood. While the X-ray–heated bubbles will still survive as fossils, once the quasar has died, the Lyα photons will rapidly adiabatically redshift out of resonance so that no emission will occur without an external supply of photons.

If reionization occurred at redshift $5 \lesssim z \lesssim 10$, these QSO spheres of influence might be detectable at meter wavelengths by the GMRT. Because of the very large scales involved, there is no difficulty in achieving a sufficiently narrow bandwidth and an adequate angular resolution with the GMRT; the main limitations are the low flux levels and the radio background subtraction.

It is possible that both the reionization and heating of the IGM were due to an early population of stars on subgalactic scales (rather than quasars) at redshift $z \gtrsim 20$, well beyond the reach of the GMRT. Even if they reionized the IGM at an epoch accessible to the GMRT, however, these sources would be less thinly spread, and the characteristic structures in the IGM generated by them would be smaller and less detectable, so that an alternative observing strategy than the one discussed here would be required.

We acknowledge helpful conversations on the subject of this paper with P. Palmer, L. Spitzer, M. Voit, W. Watson, and M. White. We thank the referee, G. Swarup, for valuable comments that helped to clarify the detectability of a neutral IGM with the GMRT. P. M. and A. M. were supported in part by NSF grant PHY 94-07194 to the ITP, University of California, Santa Barbara. A. M. is also grateful to the W. Gaertner fund for its support. M. R. thanks the Royal Society for support.

APPENDIX A

LYMAN-α LINE FLUX IN THE NEUTRAL MEDIUM

We evaluate the Lyα flux produced in the neutral H I outside an ionization front from recombinations within the H II region itself. The volume emissivity is given by

$$\epsilon_\nu = x_e\, x_p\, n_{\rm H}^2\, \alpha_{2\,^2P}^{\rm eff}\, h\nu\phi(\nu)\ , \quad (A1)$$

where $\alpha_{2\,^2P}^{\rm eff}$ is the effective recombination coefficient to the $2\ ^2P$ level (Pengelly 1964). Integrating from just outside the ionization front into the H II region, and averaging over 4π sr, we get

$$J_\alpha(r) = \frac{1}{4\pi}\int_{r_I}^{r} \epsilon_\nu\, dr \approx 1.2\alpha_{2\,^2P}^{\rm eff}\,\frac{n_{\rm H}^2\, hc}{8\pi H} \quad (A2)$$

(with $x_e = 1.2$, $x_p = 1$, and including an additional factor of $\frac{1}{2}$ since Lyα photons arise only from within the H II region). In evaluating the integral, we relate the distance $r - r_I$ from the ionization front to the frequency shift y from line center (in units of the thermal width) due to the Hubble expansion, by $r - r_I = by/H$, where b is the Doppler parameter. Because emission at

line center is quickly redshifted out of the core, only the surface of the H II region contributes to the Lyα flux. The resulting intensity can be expressed as

$$J_{\alpha,-21}(z) \approx 0.03 h_{50}^{-1} \left(\frac{\Omega_{\rm IGM} h_{50}^2}{0.05}\right)^2 \left(\frac{1+z}{7}\right)^{4.5} . \tag{A3}$$

The recombination photons escaping from an expanding H II region produce then only a small flux of Lyα photons.

For completeness, we shall also compute the contribution from the local production of Lyα photons in the warm (mostly) neutral material surrounding the ionized gas. As Lyα photons are redshifted out of the Doppler core by the Hubble expansion, the local background intensity becomes $J_\alpha = (n_{\rm H}^2 hc/4\pi H)\,[x_e x_p \alpha_{2\,2P}^{\rm eff} + x_e x_{\rm H\,I} \gamma_{\rm eH} + \mathscr{E} \dot{E}_X/(n_{\rm H} h\nu_\alpha)]$, where $\gamma_{\rm eH} \approx (2.2 \times 10^{-8}\ {\rm cm^3\ s^{-1}})\ \exp(-11.84/T_4)$ (Osterbrock 1989) is the collisional excitation rate of Lyα photons by electron impacts and the last term accounts for Lyα collisional excitations from the nonthermal distribution of electrons generated by the soft X-rays. The factor $\mathscr{E} \approx 0.4$ (Shull & van Steenberg 1985) represents the net fraction of photon energy converted to Lyα photons. For a temperature of $T_4 = 0.1$ and allowing (optimistically) for $x_e \sim x_p \sim 0.2$, radiative recombinations dominate, and

$$J_{\alpha,-21}(z) \approx 0.5 x_e x_p h_{50}^{-1} \left(\frac{\Omega_{\rm IGM} h_{50}^2}{0.05}\right)^2 \left(\frac{1+z}{7}\right)^{4.5} . \tag{A4}$$

Recombinations and collisional excitations in a warm, largely neutral medium are therefore a negligible source of Lyα photons.

APPENDIX B

HEATING BY RESONANT SCATTERING OF LYMAN-α PHOTONS

We derive the rate of transfer of energy, equation (30), from the radiation field to the atoms through recoil using the equation of radiative transfer. Neglecting expansion and source terms, the rate of change of the number density of photons in a given frequency band n_ν for an isotropic radiation field was shown by Basko (1981) to be given in the diffusion approximation by

$$\frac{1}{c}\frac{\partial n_\nu}{\partial t} = \frac{1}{2} n_{\rm H\,I} \Delta\nu_D \frac{\partial}{\partial \nu}\left[\sigma_\nu \left(\Delta\nu_D \frac{\partial n_\nu}{\partial \nu} + 2 f n_\nu\right)\right], \tag{B1}$$

where $n_{\rm H\,I}$ is the number density of hydrogen atoms in the ground state, $f = h\nu_\alpha/m_{\rm H} cb$ expresses the effect of recoil, and only terms of order v/c have been retained. This is only correct as long as $kT_K \ll h\nu_\alpha$. Note that, in a steady state, $n_\nu \propto \exp[-h(\nu - \nu_\alpha)/kT_K]$ near the resonant frequency, as was first demonstrated by Field (1959b).

The rate of change of energy in the radiation field due to recoil is then

$$\dot{u}_\alpha = h\nu_\alpha \dot{n}_\alpha = n_{\rm H\,I} c\, \Delta\nu_D\, h \int_0^\infty d\nu \nu \frac{\partial}{\partial \nu}(\sigma_\nu f n_\nu) . \tag{B2}$$

Performing the integration by parts, noting that σ_ν is sharply peaked at the resonant Lyα frequency, using $n_\nu = (4\pi/c) J_\nu/h\nu$, and setting $\dot{E}_\alpha = -\dot{u}_\alpha/n_{\rm H\,I}$, we recover equation (30) of the text. This result is valid in the presence of expansion and source terms as well, as may be shown from the generalization of equation (B1) by Rybicki & Dell'Antonio (1994). We note that, to order v/c, the flow of energy is one-directional, from the radiation field to the atoms. Treating the reverse flow requires the inclusion of terms of order $(v/c)^2$ (including relativistic effects like aberration). We have also neglected stimulated emission. These effects become particularly important when the matter approaches thermal equilibrium with the radiation field. In this limit, the radiation field relaxes to a blackbody spectrum, and the net transfer of energy ceases. In the situations relevant to this paper, these effects are negligible.

REFERENCES

Adams, T. F. 1971, ApJ, 168, 575
Allison, A. C., & Dalgarno, A. 1969, ApJ, 158, 423
Allison, A. C., & Smith, F. J. 1971, At. Data, 3, 317
Arons, J., & Wingert, D. W. 1972, ApJ, 177, 1
Bahcall, J. N., & Ekers, R. D. 1969, ApJ, 157, 1055
Bardeen, J. M., Bond, J. R., Kaiser, N., & Szalay, A. S. 1986, ApJ, 304, 15
Basko, M. M. 1981, Astrophysics, 17, 69
Bebbington, D. H. O. 1986, MNRAS, 218, 577
Bennett, C. L., et al. 1994, ApJ, 434, 587
Bergeron, J., & Souffrin, S. 1971, A&A, 11, 40
Braun, R. 1996, in Cold Gas at High Redshift, ed. M. Bremer, H. Rottgering, C. Carilli, & P. van de Werf (Dordrecht: Kluwer), 437
Couchman, H. M. P. 1985, MNRAS, 214, 137
Couchman, H. M. P., & Rees, M. J. 1986, MNRAS, 221, 53
Deguchi, S., & Watson, W. D. 1985, ApJ, 290, 578
Fabbiano, G. 1989, ARA&A, 27, 87
Field, G. B. 1958, Proc. IRE, 46, 240
Field, G. B. 1959a, ApJ, 129, 536
———. 1959b, ApJ, 129, 551
Gallego, J., Zamorano, J., Aragón-Salamanca, A., & Rego, M. 1995, ApJ, 455, L1
Górski, K. M., Ratra, B., Sugiyama, N., & Banday, A. J. 1995, ApJ, 444, L65
Gould, R. J., & Thakur, R. K. 1970, Ann. Phys., 61, 351
Gunn, J. E., & Peterson, B. A. 1965, ApJ, 142, 1633
Hogan, C. J., & Rees, M. J. 1979, MNRAS, 188, 791
Hu, W., & White, M. 1996, A&A, in press
Longair, M. S. 1995, in Extragalactic Background Radiation, ed. D. Calzetti, M. Livio, & P. Madau (Cambridge: Cambridge Univ. Press), 223
Madau, P., & Meiksin, A. 1991, ApJ, 374, 6
———. 1994, ApJ, 433, L53
Madau, P., & Shull, J. M. 1996, ApJ, 457, 551
Mather, J. C., et al. 1994, ApJ, 420, 439
Meiksin, A. 1994, ApJ, 431, 109

Meiksin, A., & Madau, P. 1993, ApJ, 412, 34
Miralda-Escudé, J., & Rees, M. J. 1994, MNRAS, 266, 343
Moiseiwitsch, B. L. 1962, in Atomic and Molecular Processes, ed. D. R. Bates (New York: Academic Press), 280
Osterbrock, D. E. 1989, Astrophysics of Gaseous Nebulae and Active Galactic Nuclei (Mill Valley: University Science Books)
Peebles, P. J. E. 1993, Principles of Physical Cosmology (Princeton: Princeton Univ. Press)
Pengelly, R. M. 1964, MNRAS, 127, 145
Phinney, E. S. 1985, Astrophysics of Active Galaxies and QSOs, ed. J. S. Miller (Oxford: Oxford Univ. Press), 453
Press, W. H., & Schechter, P. 1974, ApJ, 187, 425
Purcell, E. M., & Field, G. B. 1956, ApJ, 124, 542
Rees, M. J. 1985, MNRAS, 213, 75P
Rybicki, G. B., & Dell'Antonio, I. P. 1994, ApJ, 427, 603
Schneider, D. P., Schmidt, M., & Gunn, J. E. 1991, AJ, 101, 2004
Scott, D., & Rees, M. J. 1990, MNRAS, 247, 510
Shapiro, P. R. 1986, PASP, 98, 1014
Shull, J. M., & van Steenberg, M. E. 1985, ApJ, 298, 268
Spitzer, L. 1962, Diffuse Matter in Space (New York: Wiley)
———. 1978, Physical Processes in the Interstellar Medium (New York: Wiley)
Spitzer, L., & Scott, E. H. 1969, ApJ, 158, 161
Subramanian, K., & Padmanabhan, T. 1993, MNRAS, 265, 101
Sugiyama, N., Silk, J., & Vittorio, N. 1993, ApJ, 419, L1
Swarup, G. 1996, in Cold Gas at High Redshift, ed. M. Bremer, H. Rottgering, C. Carilli, & P. van de Werf (Dordrecht: Kluwer), 457
Swarup, G., Ananthakrishan, S., Kapahi, V. K., Rao, A. P., Subrahmanya, C. R., & Kulkarni, V. K. 1991, Curr. Sci., 60, 95
Swarup, G., & Malik, R. K. 1996, private communication
Urbaniak, J. J., & Wolfe, A. M. 1981, ApJ, 244, 406
Warren, S. J., Hewett, P. C., & Osmer, P. S. 1994, ApJ, 421, 412
White, S. D. M., Efstathiou, G., & Frenk, C. S. 1993, MNRAS, 262, 1023
Wouthuysen, S. A. 1952, AJ, 57, 31